NAILED MORTISED-PLATE CONNECTIONS FOR SMALL-DIAMETER ROUND TIMBER[1]

*Kug-Bo Shim**

Research Scientist
Department of Forest Products
Korea Forest Research Institute
Seoul, 130-712, Korea

Ronald W. Wolfe

General Engineer

Marshall Begel

Structural Engineer, PE
Engineering Mechanics Laboratory
USDA Forest Products Laboratory
1 Gifford Pinchot Drive
Madison, WI 53726

(Received January 2009)

Abstract. In an effort to encourage the development of value-added engineered applications for small-diameter round timber, research is being conducted at the US Forest Products Laboratory to develop and verify design guidelines for connections with specific application to round timbers. The objective of this study is to provide potential users with a number of viable connection options applicable to the fabrication of engineered, round-timber structural components and systems. Target uses include trusses, built-up flange beams, and space frames. This article presents information on a mortised steel-plate connection fabricated using power-driven nails in 150-mm-dia ponderosa pine. The article discusses methods used to determine per nail load capacity and to develop design procedures that incorporate that value in the determination of a multinail connection design value. These connections offer the advantage of low labor and material cost, ductile failure modes, and strengths in the range of 4.7 kN/nail. The failure of the connections was mode III nail failure and wood block shear failure. Joints that failed in block shear appeared to have roughly the same strength as those that failed from nail yield. The National Design Specification yield model for nails provides accurate predictions of joint capacity for nail yield-type failures and overestimates strength of joints that exhibit wood failure. Block shear capacity can be estimated on the basis of clear-wood strength and effective tensile and shear area of the connection.

Keywords: Small-diameter round timber, connections, power-driven nails, design value, failure mode.

INTRODUCTION

There are many advantages of using small-diameter timber structurally in the round form (Wolfe 2000). In cutting a small-diameter ponderosa pine log into dimension lumber, roughly 60% of the log converts to low or no value slabs, chips, and sawdust. The economic value of this waste material varies with the capabilities of the local infrastructure. In terms of the engineering value, however, the material taken off as slab contains the best wood. In the round form, these timbers have approximately five times the beam load capacity and twice the column capacity of the largest rectangular timber that can be cut from them. In its raw, debarked form, the log will exhibit less drying degrade as a result of unsymmetric distribution of juvenile wood than sawn lumber and provides superior fire resistance as a result of a smaller surface-to-volume ratio than dimension lumber.

* Corresponding author: kbshim@forest.go.kr

To expand the market for these logs beyond the limits of simple beams, columns, or wall logs, methods must be developed for their incorporation in built-up engineered components and systems. Examples include log trusses, the round timber version of the I-joist, referred to as an 8-beam, built-up column, and space frame systems. These applications can be designed to avoid problems with the round shape and taper, and the net section properties can be adjusted to expand span capabilities. The primary barrier to incorporating round timber into engineered components is the limited selection of applicable commodity market connections. Commercially produced spike grids provide for transfer of shear between lapped round wood and dimension lumber elements. There are, however, no recognized design standards for in-line connections designed to transfer axial forces or bending moments between round timbers. To expand the structural market for round timbers, a variety of connection options are needed along with the appropriate load capacity prediction models (Shim and Lee 2005). Research is needed to evaluate the efficacy of a variety of connection systems and to assess their performance under a variety of potential environmental as well as structural load conditions.

This article presents an evaluation of nailed mortised-plate connections as a possible solution to the connection problem that limits development of round timber structural components. Tests were conducted to provide a basis for assigning single-nail values for mode III and mode IV type nail failures as well as for predicting block shear failure in the wood. These results were used to predict the capacity and failure mode of multinail connections and to provide a basis for comparing this connection with other joints. This study is focused on nailed connections in round ponderosa pine timbers. These connections incorporate plate steel to transfer axial loads between round timber elements. The joint configuration studied in this report incorporates a steel plate, which is placed in a slot cut parallel to the log diameter but one-half of the nail length from the outer surface. In this case, the nail is loaded in double shear. For this study, connection tests were limited to axial tension. Although the joint itself carries an axial load, the failure mechanism involved bearing forces parallel to the grain and a shear/bending load on the nails up to the nail density to cause block shear failures in the wood. Variables considered the number of nails and nail density up to the point of wood block shear failure. Modeling parameters developed to predict the performance of these connections under axial load can be modified to predict performance when loaded perpendicular to the grain, but this failure mode was not tested as part of the study.

METHODS

Nailed plate connections were tested to assess the predictability of multinail connections. Variables included the number of nails and spacing of the nails parallel to the grain. All other parameters were held constant. The test series was conducted using 13 logs with six different joint configurations fabricated and tested for each log. This sample was considered sufficient to evaluate mean strength and per nail sensitivity to nail pattern and number of nails.

Test Joint Fabrication

The joints tested consisted of round timber members with two mortised steel plates locked in place using hardened steel nails, which were driven using a powder-actuated gun driver (Hilti model DXA41). Ponderosa pine timbers, peeled to a uniform 150-mm dia, were kiln-dried and stored in a 12% MC conditioning room for a minimum of 3 mo before the initial joint fabrication. The logs were initially cut and dried in 2.4-m lengths. Each log was cut into two sections and a dowel-nut connection was attached to one end. The free end was then machined to receive the mortised plates (Fig 1). Because test loads were well below the capacity of the timber, failed portions were removed to produce subsequent end-matched tests in material that was not influenced by the previous failures.

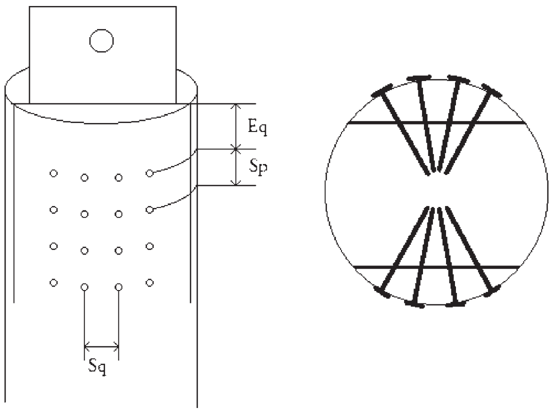

Figure 1. Configurations of power-driven nail connection.

The nail patterns were generally rectangular. In referring to these patterns, the lines of nails oriented parallel to the grain are referred to as rows and those perpendicular to the grain are columns. The spacing between rows, distance perpendicular to the grain, is designated S_q and spacing parallel to the grain is S_p. This notation is shown in Fig 2.

Test Procedure

Tests were initially conducted to obtain strength and stiffness of the nails. These tests were conducted following the procedures given in ASTM F1575 (ASTM 2003) for determining yield moment of nails.

Figure 3 shows the test joint setup. A screw-type test machine was used to apply an axial tension load at a load head displacement of 2.5 mm/min. At this rate, the maximum load was reached in 5 – 10 min. Loads were measured using a 220-kN load cell and a single linear variable differential transformer (LVDT) was used to measure average displacement of the plates with respect to the end of the log. Load and displacement data were digitally recorded and stored for each joint.

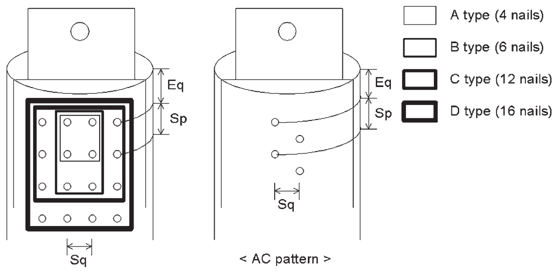

Figure 2. Nail patterns for power-driven nail connection.

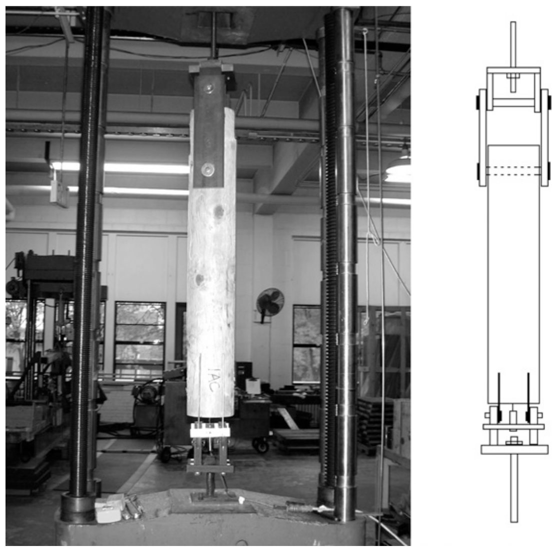

Figure 3. The test joint setup.

RESULTS

Material Properties

Log properties vary from the center to the outer surface; therefore, the outer portion of the nail resists more load than the inner portion. The specific gravities ranged from 0.37 – 0.48 in the outer part of the logs, whereas samples taken close to the pith ranged from 0.31 – 0.48. In both cases, the average value was 0.42, but there was greater variability among the inner samples. Growth rate averaged 6.3 rings/mm in the outer part and 3.3 rings/mm close to the pith, but there was no apparent correlation between growth rate and density. Nail tests were conducted following ASTM F1575. Ten tests gave almost identical results. Using a 5% offset secant to define a yield stress, the test showed an average yield load of 1.66 kN, which corresponds to a yield stress of 1.86 GPa. This is virtually the same as values published by Hilti (1.85 GPa).

Connection Failures

Connections are designed on the basis of their load capacity, which is a function of material properties, joint configuration, and the load and boundary conditions. Another important consideration, however, is failure ductility. In the rare event that the load on an engineered structure exceeds the capacity, it is desirable that the structure continues to support load as it deforms. This property can be quantified as the area under the load displacement curve beyond the point of maximum load. Figures 4 and 5 illustrate the extremes of ductile behavior. These are load displacement plots for two connections of the same basic configuration. Figure 4 shows what occurs beyond the yield load, 72 kN, when energy is dissipated in the form of nail bending and wood bearing deformation. Figure 5, by comparison, shows an increase in load beyond yield (60 kN) to a capacity of 100 kN at 2 mm displacement followed by an abrupt drop in load capacity as a result of splitting or a tensile fracture. Although those both tests had the same basic configuration, they exhibited different failure mechanisms and different ductility.

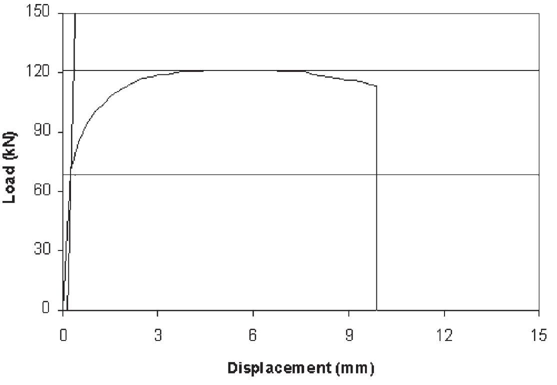

Figure 4. Load displacement curve for ductile failure.

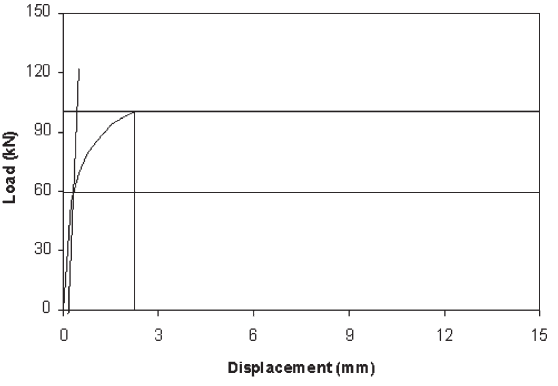

Figure 5. Load displacement failure for brash failure.

Failure mechanisms are broadly classified as nail vs wood failures. Nail failures involve displacement of the nail relative to the wood in the form of lateral displacement, bending, or rotation. This is accompanied by bearing deformation in the wood and ultimately either splitting of the wood or lateral nail withdrawal. Nail failures are further classified into "modes" (AF&PA 2005) depending on the combination of nail and wood deformation. The nail failures observed in this study were primarily of mode 3 in which the nails exhibit one bending per shear plane (Fig 6). Wood failures are characterized by breaking of wood fiber in some combination of shear, tension, or bending. When the nail density was sufficient to exceed the shear strength of the wood on either side of the nail pattern, shear and ultimately tension fractures appeared, and a block of wood containing the nail pattern was pulled away. This was labeled as a "block shear" failure (Fig 7).

Loading the connections beyond the maximum load caused several additional failure mechanisms, but these did not appear to have an influence on joint capacity. One of these appears as a wood failure pattern best described as cleavage. The other, caused by a stiffer connection between the plate and the mature outer wood, appeared as an outward rotation of the plate, opening the mortise slot at the end of the log and imposing bending stresses on the outer wood at the base of the mortise cut. The cleavage or longitudinal splits corresponding to the nail rows appeared on the wood surface where the nail heads had been pulled into the surface and parallel to the grain forcing the wood apart in tension perpendicular to the grain. This pattern appeared in all nail patterns, but the fact that the nails were bent suggests that this fracturing of the wood occurred after the maximum

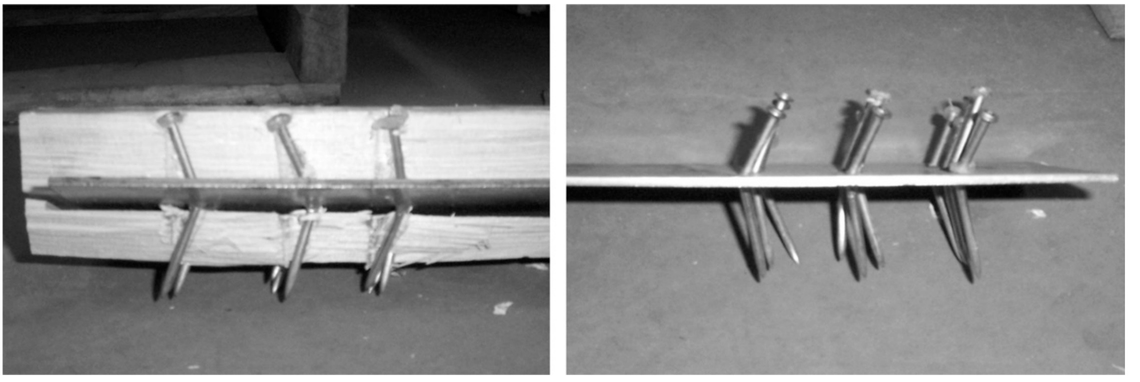

Figure 6. Mode III nail bending failure.

Figure 7. Block shear failures.

load was reached. In a few instances, some of the nails were not bent, suggesting that the splits were present before the test, possibly from drying. For tests in which the splitting did not occur, the greater resistance of the nail head to being drawn through the wood resulted in an eccentric load on the plate, causing it to rotate outward at the top. Because this was associated with deformation beyond the joint yield limit, it had little effect on connection yield or ultimate strength. Maximum loads measured for the various test connections are shown in Table 1.

ANALYSIS OF RESULTS

Connections are generally designed to carry a load, which is roughly one-third of the ultimate value or one-half of the yield strength. Timber rivets are evaluated as the ultimate strength divided by 3.3. This divisor is intended to account for duration of load, factor of safety, and variability. The National Design Specification (NDS) for Wood references the European yield model for nails, which uses a factor of 1/2.2 times the yield strength (5% offset) as a basis for design. In addition to evaluating the test results at maximum load (Table 1), yield strengths were evaluated for each curve by modeling each using a hyperbolic tangent model. The first derivative of this model was used to define a secant slope between 20 – 40% of the maximum load. This slope and an intercept equal to 0.05 times the nail diameter defined a line whose intersection with the hyperbolic tangent model defined the yield strength (P_y) and displacement (D_y).

Table 1. *Maximum load (kN) for the test joint configurations.*

Specimen number	AA	AB	AC	BB	CB	DB
1	40.2	43.7	44.9	64.5	127.7	121.9
2	35.6	37.9	39.1	49.5	—	—
3	42.5	40.7	39.1	55.2	103.5	145.2
4	37.2	42.1	41.1	57.5	120.5	134.4
5	33.0	33.9	35.9	48.8	117.0	121.9
6	35.5	40.5	37.8	55.4	104.0	—
7	41.0	41.2	41.1	60.4	95.0	115.8
8	36.6	38.0	39.0	55.3	100.5	107.2
9	34.1	44.0	32.2	68.9	112.5	—
10	43.5	—	40.3	—	100.8	—
11	40.8	40.0	43.0	58.7	125.6	—
12	—	44.4	32.8	59.4	121.7	151.9
13	39.1	32.8	36.9	47.1	97.8	114.8
No. of Nails	8	8	8	12	24	32
Nr =	2	2	2	2	4	4
Nc =	2	2	2	3	3	4
Sq (mm) =	25.4	25.4	25.4	25.4	25.4	25.4
Sp (mm) =	25.4	38.1	38.1*	38.1	38.1	38.1

* Staggered rows.

Connection Models

For purposes of simplification, failure of the test connections has been attributed to one of two failure mechanisms: nail bearing or wood rupture. Wood failures comprised a combination of shear and tension failure in the wood, which formed the perimeter of the connection block. Failures of the four- and six-nail/plate connections were all attributed to nail yield and wood bearing deformation. Wood failure played a significant role in defining capacity of the 12- and 16-nail/plate connections.

Two analytical models, derived to predict connection capacity, were evaluated and compared with the test data. The nail yield model (AF&PA 2005) for mode III failures was compared with a wood failure model, which relates connection strength to clear wood strength (ASTM D2555; ASTM 1998) and connection geometry.

Nail yield model. The nail yield model (AF&PA 2005) provides a prediction of design load, which should be equal to 45% of the yield value. The NDS equation for mode III failures is:

$$Z = \frac{k_2 \times D \times t_s \times F_{em}}{K_D \times (2 + R_e)} \qquad (1)$$

where

$$k_2 = -1 + \sqrt{\frac{2 \times (1 + R_e)}{R_e} + \frac{2 \times F_{yb} \times (2 + R_e) \times D^2}{3 \times F_{em} \times t_s^2}}$$

R_e = F_{em}/F_{es} = 0.078;
t_s = thickness of side member (1.59 mm);
F_{em} = dowel bearing strength of main member (holding point) (24 MPa);
F_{es} = dowel bearing strength of side member (310 MPa);
F_{yb} = bending yield strength of nail or spike (1.67 GPa);
D = nail or spike diameter (3.7 mm); and
K_D = 2.2.

This equation yields a design capacity of 695 N under a mode III failure. The mortised plate detail causes each nail to be loaded in double shear giving a per nail design capacity of 2 × Z or 1390 N. Multiplying this by 2.2 gives an estimated yield strength of 3.06 kN.

Wood failure model. The wood failure mode basically estimates the shear and tensile capacities of wood planes that surround the wood block volume as defined by the area and depth of the nailing pattern. The cross-section of this block is viewed as a portion of a sector of a hollow cylinder (Fig 8) having an outer radius equal to that of the timber (*r*) and an inner radius equal to r minus the nail length. This sector is split into two parts by the 3.2-mm-thick mortise oriented perpendicular to the center radius of the sector and located midway between the inner and outer surfaces. The nails are assumed to be driven in the radial direction so that the width of the nail pattern on the log surface defines the angle (θ) of the sector. This block extends from the end of the timber to the most distant column of nails.

The cross-section of this sector defines the tensile surface. Eq 2 estimates the net effective tensile area as that area outside the mortise. The nail points came together inside the mortise. This combined with the fact that this area

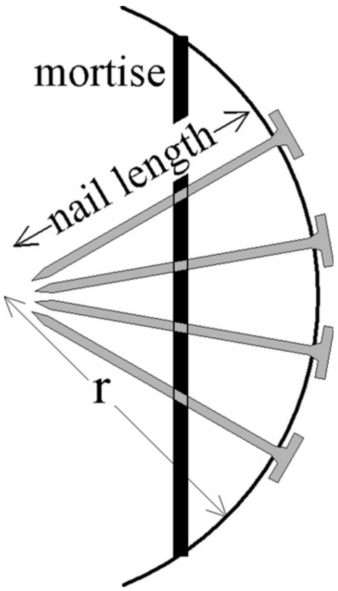

Figure 8. Tensile area of the power-driven nail connection.

consists primarily of juvenile wood fiber effectively reduces its tensile contribution. Eq 2 also accounts for the projected areas of the nails and an allowable knot on the tensile plane outside the mortise.

A_t = sector area – pith-to-plate area – nail hole area – projected knot area

$$A_T = \left[\frac{r^2 \times \theta}{2} - [(r - (l_p - t_s)) \times 0.5]^2 \times TAN\left(\frac{\theta}{2}\right) - D_n \times \frac{l_p - t_s}{2} \times N_R - A_k\right] \times 2 \quad (2)$$

where

$$\theta = \frac{(N_R - 1) * S_q}{r}$$

$$A_k = 0.5 \times r \times D_k - [r - (l_p - t_s) \times 0.5]^2 \times TAN\left(\frac{D_k}{2 \times r}\right)$$

A_T = tensile area of a shear block outside the mortise (mm^2);
A_k = knot area projected on A_T (mm^2);
D_k = allowable knot diameter (mm);
D_n = nail diameter (mm);
L_p = penetration length of the nail into the wood (72 mm);
r = log radius (76 mm);
θ = sector angle defined by the nail pattern;
t_s = thickness of the mortise (3 mm);
N_R = number of nail rows; and
S_q = distance between rows (25 mm).

The effective shear area (A_V) is given by Eq 3. The connection includes four shear planes, each defined by the nail penetration length (l_p) times the length from the end of the timber to the end of the nail pattern. The cross-sectional areas of the mortise and the nails, which penetrate the shear planes, are subtracted. Eq 3 also includes an adjustment (k) for the ratio of juvenile wood strength. Assuming that one-half of each shear plane is in juvenile wood, the effective area is $0.5 \times (1 + k)$ of the net area.

$$A_V = 4 \times [(L_p - t_s) \times ((N_C - 1) \times S_p + e_p) - D_n \times l_p \times Nc] \times 0.5 \times (1 + k) \quad (3)$$

where

A_V = total shear area (mm^2);
N_C = number of nail columns (oriented perpendicular to the grain);
S_p = distance between columns (mm);
e_p = distance from the end of the timber to the first column of nails (mm); and
k = ratio of juvenile wood shear strength to mature wood shear strength.

As discussed earlier, the wood block shear failure consisted of both shear and tension failures. However, these were not additive. The estimated shear strength alone, assuming a 20% reduction for juvenile wood, provides a fairly close estimate of ultimate capacity for the CB and DB connections. The strength of the gross tensile area, however, is greater than the measured joint strength. For ponderosa pine, the published values for tensile strength and stiffness are roughly eight times that of shear

Table 2. *The average measured and predicted yield loads and design values for the tested connections.*

	AA	AB	AC	BB	CB Nail bend	CB Block shear	DB Nail bend	DB Block shear
Yield load (kN)								
Measured	22.9	25.1	25.2	37.1	73.2	72.0	91.4	90.1
SD	2.09	2.80	2.63	3.78	5.52	10.99	9.61	4.05
D_y (mm)	0.69	0.48	0.41	0.41	0.41	0.36	0.23	0.33
Predicted	25	25	25	37	73	73	91	91
Design value (yield load/2.2)								
Measured	11	12	12	17	33	33	42	41
Predicted	11	11	11	17	33	33	39	39
Per nail design value								
Measured	1.37	1.5	1.5	1.4	1.37	1.37	1.31	1.28
Predicted	1.39	1.39	1.39	1.39	1.39	1.39	1.20	1.20

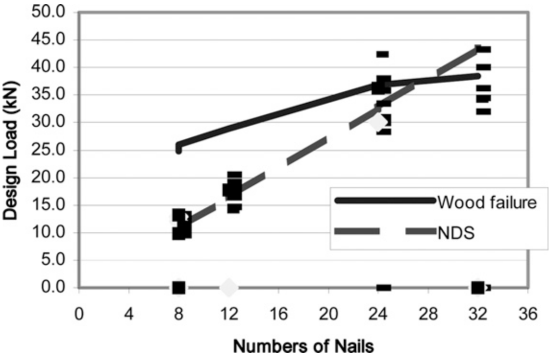

Figure 9. The design load comparison between wood failure and nail bending (NDS).

(FPL 1999). The relatively low shear stiffness and long shear planes suggest an accumulation of shear strain along the edges of the shear block would lead to progressive failure and that ultimate load would be controlled by the tensile strength. Therefore, rather than ignoring tension and attributing the load capacity to shear alone, we chose to assess the wood failure as a combination of tension and shear. Because tension strength was greater than shear in most cases, it was considered to be the primary consideration for joint strength prediction under a wood failure mode. The shear contribution is assumed to be dependent on the ratio of shear area to tensile area. The greater the shear area, the longer the shear length and the greater the shear contribution. If the connection details were such that shear capacity was much greater than tension, it is likely that shear would become the controlling influence on connection capacity. However, there were insufficient data to fully develop this relationship. Eq 4 provides the design load predictions shown in Fig 9 and the limiting design values for the DB connection detail (Table 2). Design load based on wood failure model predictions divided by 3.36 exceeds that predicted using the NDS nail yield and the test data for the 8 and 12 nail joints but is close to the mean strength of the 32 nail joints.

$$P_{ult} = F_t \times A_t + \left(\frac{A_v}{A_t \times L_v}\right) \times \beta \times F_v \times A_v \quad (4)$$

where β is an empirically derived value of 0.06.

CONCLUSIONS

The objective of this study is to provide the information on a mortised steel plate connection fabricated using powder-driven nails for 150-mm-dia ponderosa pine round timber. This type of connection is a viable option applicable to the fabrication of engineered, round-wood structural components and systems. Conclusions are as follows:

1. The average maximum load per nail was roughly 4.7 kN for connections exhibiting a mode III nail failure.
2. Joints that failed in block shear appeared to have roughly the same strength as those that failed from nail yield.

3. The NDS yield model for nails provides accurate predictions of joint capacity for nail yield type failures and overestimates strength of joints that exhibit wood failure.
4. Block shear capacity can be estimated on the basis of clear-wood strength and effective tensile and shear area of the connection.

ACKNOWLEDGMENTS

The study on the use of powder-driven fasteners was funded through a grant from USDA. The equipment for manufacturing the test joints was contributed to the study, along with training on its use and maintenance by the US division of Hilti Inc., Tulsa, OK.

REFERENCES

AF&PA (2005) National design specification for wood construction. American Forest and Paper Association. Washington, DC.

ASTM (1998) D2555. Standard test method for establishing clear wood strength values. American Society for Testing and Materials, West Conshohocken, PA.

——— (2003) F1575. Standard test method for determining bending yield moment of nails. American Society for Testing and Materials, West Conshohocken, PA.

FPL (1999) Wood handbook—Wood as an engineering material. USDA For Serv Forest Products Laboratory, Madison, WI.

Shim K-B, Lee D-S (2005) The tensile properties for power-driven-nail connections for Japanese Larch small round timber. J Korean Wood Sci Technol 33(2):8 – 16.

Wolfe R (2000) Research challenges for structural use of small-diameter round timbers. Forest Prod J 50(2): 21 – 29.